

**Creation and mobility of discrete solitons in Bose-Einstein condensates**

V. Ahufinger,<sup>1</sup> A. Sanpera,<sup>1</sup> P. Pedri,<sup>1,2</sup> L. Santos,<sup>1</sup> and M. Lewenstein<sup>1</sup>  
<sup>1</sup>*Institut für Theoretische Physik, Universität Hannover, D-30167 Hannover, Germany*  
<sup>2</sup>*Dipartimento di Fisica, Università di Trento and BEC-INFN, I-38050 Povo, Italy*

(Received 2 October 2003; published 6 May 2004)

We analyze the generation and mobility of discrete solitons in Bose-Einstein condensates confined in an optical lattice under realistic experimental conditions. We discuss first the creation of one-dimensional discrete solitons, for both attractive and repulsive interatomic interactions. We then address the issue of their mobility, focusing our attention on the conditions for the experimental observability of the Peierls-Nabarro barrier. Finally we report on the generation of self-trapped structures in two and three dimensions. Discrete solitons may open alternative routes for the manipulation and transport of Bose-Einstein condensates.

DOI: 10.1103/PhysRevA.69.053604

PACS number(s): 03.75.Lm, 03.75.Kk, 05.30.Jp

**I. INTRODUCTION**

The experimental achievement of the Bose-Einstein condensate (BEC) [1] has outbursted an extraordinary interest within the last years in the physics of ultracold atomic gases. This interest can be partially explained by the inherently nonlinear character of the BEC physics induced by the interatomic interactions. At sufficiently low temperatures, the physics of the condensates is governed by a nonlinear Schrödinger equation with cubic nonlinearity, also called Gross-Pitaevskii equation (GPE), similar as that encountered in other physical systems, as e.g., nonlinear optics (NLO) in Kerr media. The analysis of the resemblances between BEC physics and NLO has lead to the rapidly developing field of nonlinear atom optics (NLAO) [2]. Recently, several experiments have highlighted various NLAO phenomena, as dark solitons in BEC with repulsive interatomic interactions [3,4], bright solitons in one-dimensional (1D) BECs with attractive interactions [5,6], and condensate collapse [7].

During the last few years, the possibility of loading a BEC in an optical lattice formed by a laser standing wave has attracted considerable attention, mostly motivated by the close resemblance between these systems and solid-state devices. In this sense, several remarkable experiments have been recently reported, as the observation of Bloch oscillations of BECs [8,9], the realization of Josephson-junction arrays of BECs placed in different lattice sites [10], or even the achievement of the superfluid to Mott-Insulator transition [11]. Recently, several nonlinear BEC phenomena have been analyzed in the presence of optical lattices, as the dynamical superfluid to insulator transition [12], the BEC transport in the presence of dispersion managing [13], and the generation of gap solitons, i.e., bright solitons with condensates with repulsive interactions [14,15].

Particular interest has been recently devoted to those phenomena occurring when the condensate dimensions become comparable to the lattice wavelength. In that case, the discrete structure introduced by the lattice potential may lead to similar phenomena as those observed in NLO in periodic structures. In particular the analysis of discrete solitons (DS) [16–18] in the BEC context has recently attracted a growing attention [19–23]. Specially interesting phenomena exclusively induced by the discreteness of the system have been

analyzed in the NLO context, such as the restriction of the mobility of the DSs due to the so-called Peierls-Nabarro (PN) barrier [24], or the possibility to generate two-dimensional DSs [25].

Although several properties related with DSs in BEC have been already reported [19–21], the realization of DSs under realistic experimental conditions has so far not been analyzed in detail. Therefore, one of the aims of the present paper is to discuss the creation of these structures in the frame of the recent experiments on BEC in optical lattices. In particular, we shall discuss the generation of 1D DS for both attractive and repulsive interacting condensates. Once created, the effects of the discrete nature of the DSs in BEC should be analyzed by means of the observation of the PN barrier for its mobility. A second aim of the present paper is to discuss the conditions for the experimental observability of this barrier. Interestingly, the PN barrier is largely overestimated within the usual tight-binding approximation even under conditions for which this approximation is typically assumed. Finally, in the last part of our paper, we discuss the possibility of achieving 2D and even 3D self-trapped structures, which could offer alternative routes for the controllable manipulation of BECs.

The scheme of the paper is as follows. In Sec. II we discuss the physical system under consideration as well as the basic equations to describe it. Section III presents a variational approach which allows for an analysis of discrete structures in arbitrary dimensions. Section IV is devoted to the analysis of the generation of 1D DSs, for both attractive and repulsive interatomic interactions. We address also in Sec. IV the issue of their mobility and provide the conditions for the observability of the Peierls-Nabarro barrier. In Sec. V we analyze the creation of 2D and 3D self-trapped structures. We finalize in Sec. VI with our conclusions.

**II. PHYSICAL SYSTEM**

In the following we consider a trapped BEC in the presence of an optical lattice. The periodic structure leads to an energy-band structure [26–29], and strongly modifies the dynamics of the condensate [8–10,12–15,30]. In the mean-field approximation, the full BEC dynamics (at a temperature

much smaller than the critical one for the condensation) is governed by the time-dependent GPE:

$$i\hbar \frac{d\psi(\vec{r},t)}{dt} = \left( -\frac{\hbar^2}{2m} \Delta + V(\vec{r}) + g|\psi(\vec{r},t)|^2 \right) \psi(\vec{r},t), \quad (1)$$

where  $g=4\pi\hbar^2 a/m$ , with  $a$  as the  $s$ -wave scattering length and  $m$  the atomic mass. The condensate wave function is normalized to the total number of particles  $N$ . The external potential is given by

$$V(\vec{r}) = \frac{m}{2}(\omega_x^2 x^2 + \omega_y^2 y^2 + \omega_z^2 z^2) + V_0 \left[ \sin^2\left(\frac{\pi x}{d}\right) + \sin^2\left(\frac{\pi y}{d}\right) + \sin^2\left(\frac{\pi z}{d}\right) \right], \quad (2)$$

which describes both the magnetic trap potential and the optical lattice (created by two counter propagating laser beams of wavelength  $\lambda$  along each axis). The angular frequencies of the magnetic trap in each direction are denoted by  $\omega_i$ . The optical lattice is characterized by its depth  $V_0$  and by its lattice period  $d=\lambda/2$ , which defines the so-called recoil momentum  $k_r=\pi/d$ . In the following, and following the standard notation, we refer the depth of the optical potential in units of the so-called recoil energy  $E_r=\hbar^2 k_r^2/2m$ .

When the optical depth of the lattice is much larger than the chemical potential ( $V_0 \gg \mu$ ), and the system can be considered as confined within the lowest energy band, one can employ the tight-binding approximation and rewrite the condensate order parameter as a sum of wave functions localized in each well of the periodic potential:

$$\psi(\vec{r},t) = \sqrt{N} \sum_n \phi_n(t) \varphi_n(\vec{r}), \quad (3)$$

where  $\varphi_n(\vec{r}) = \varphi(\vec{r}-\vec{r}_n)$  denotes the on-site wave function. By inserting the ansatz (3) into Eq. (1), one obtains that the GPE reduces to a discrete nonlinear Schrödinger equation (DNLSE):

$$i\hbar \frac{\partial \phi_n}{\partial t} = -J(\phi_{n-1} + \phi_{n+1}) + (\epsilon_n + U|\phi_n|^2)\phi_n. \quad (4)$$

The dynamics of the system depends mostly on the interplay between the tunneling rate ( $J$ ) and the two-body interactions (nonlinear energy,  $U$ ). The tunneling rate can be expressed as

$$J = - \int d\vec{r} \left[ \frac{\hbar^2}{2m} \vec{\nabla} \varphi_n \vec{\nabla} \varphi_{n+1} + \varphi_n V(\vec{r}) \varphi_{n+1} \right]. \quad (5)$$

The nonlinear term acquires the form

$$U = gN \int d\vec{r} \varphi_n^4 \quad (6)$$

and the on-site energies are given by

$$\epsilon_n = \int d\vec{r} \left[ \frac{\hbar^2}{2m} (\vec{\nabla} \varphi_n)^2 + V(\vec{r}) \varphi_n^2 \right]. \quad (7)$$

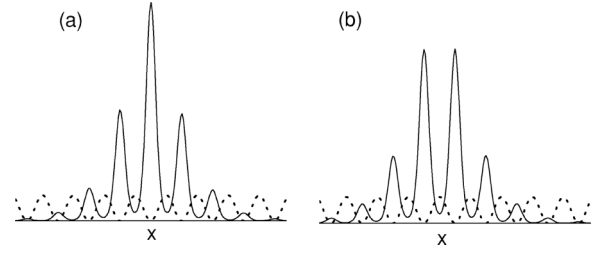


FIG. 1. Density profile of a discrete soliton (solid line) with (a) the center of mass centered in one minimum of the optical lattice and (b) the center of mass displaced by half lattice period.

In order to calculate the value of the nonlinear energy Eq. (6), we use a Gaussian ansatz for the wave function on site, where the width is obtained by minimization of the energy [31]. In the pure one-dimensional case, we use the interaction constant obtained by averaging the 3D coupling constant over the radial density profile [32]. To calculate the tunneling rate, the same Gaussian ansatz can be employed in Eq. (5) or, in the limit  $V_0 \gg E_r$ , it can be obtained from the exact result for the width of the lowest band in the 1D Mathieu equation [33].

### III. VARIATIONAL CALCULATION

Discrete solitons are characterized by being stable solutions of the Hamiltonian which propagate without distortion. They correspond to minima of the energy of the system which in the tight-binding approximation acquires the form

$$E = \sum_{n=-\infty}^{\infty} \left\{ -J\phi_n^*(\phi_{n-1} + \phi_{n+1}) + \epsilon_n |\phi_n|^2 + \frac{U}{2} |\phi_n|^4 \right\}. \quad (8)$$

Let us consider first the 1D case. To find the minima of the energy, an exponential ansatz for the soliton envelope given by  $\phi_n = C \exp(-\beta|n|)$  can be employed, where  $C$  is a normalization constant and  $\beta$  is a variational parameter which accounts for the inverse width of the soliton. Introducing this ansatz in Eq. (8) the expression for the energy, in the negative scattering length case, becomes

$$\frac{E}{|U|} = -\frac{4J}{|U|} \frac{e^\beta}{e^{2\beta} + 1} - \frac{1}{2} \frac{(e^{2\beta} - 1)(e^{4\beta} + 1)}{(e^{2\beta} + 1)^3}. \quad (9)$$

By minimizing  $E$  with respect to the inverse width  $\beta$  one obtains the energy of the discrete structure centered in one minimum of the optical lattice [Fig. 1(a)]. Notice that in order to ensure that the discrete structure corresponding to this minimum is indeed a soliton, one has to address the issue of its mobility. In contrast with the case of continuous solitons where applying an external momentum results in a linear response of the soliton, in discrete systems a similar effect occurs only for broad soliton distributions (i.e., those that occupy many sites). Conversely if the dimensions of the soliton are of the order of the lattice wavelength  $\lambda$  the discreteness of the system begins to play a fundamental role. In particular, the discreteness generates an effective periodic potential energy, whose amplitude is the minimum barrier which must be overcome to translate the center of mass of

the system half a lattice period, i.e., from one minimum of the lattice [Fig. 1(a)] to a neighboring lattice maximum [Fig. 1(b)]. This is the previously mentioned PN barrier [24]. The energy of the state depicted in Fig. 1(b) can be also calculated within a variational approach using

$$\phi_n = C \exp\left(-\beta \left|n - \frac{1}{2}\right|\right)$$

as an ansatz:

$$\frac{E}{|U|} = -\frac{2J}{|U|} \frac{[1 + \sinh(\beta)]}{e^\beta} - \frac{1}{4} \frac{(e^{2\beta} - 1)}{(e^{2\beta} + 1)}. \quad (10)$$

Again by minimization one obtains the energy of the displaced discrete structure. The difference between both energies [minima of Eqs. (9) and (10)] corresponds to the PN barrier.

Notice that the barrier becomes relevant when the soliton structure occupies few sites of the lattice. By increasing the number of occupied states the above two modes approach in energy and the barrier decreases approaching zero as the number of sites grows. In this sense, the PN barrier is a distinctive discrete phenomenon.

The above analysis can be straightforwardly generalized to higher dimensions. Assuming the most general case, in which the width of the exponential ansatz along the direction of the movement is different from the other directions, it can be shown that localized structures are also possible in two and three dimensions under an appropriate ratio between tunneling and nonlinear energy (see Sec. V). A variational calculation using a Gaussian ansatz instead of the exponential one has also been performed obtaining equivalent results.

#### IV. GENERATION AND MOVEMENT OF ONE-DIMENSIONAL DISCRETE SOLITONS

In this section we analyze the issue of the generation and mobility of DSs in 1D BEC under realistic experimental conditions. Let us first discuss the generation of DSs in condensates with positive scattering length. In particular, we consider a  $^{87}\text{Rb}$  condensate held in a magnetic trap and in the presence of an optical lattice. As discussed in Refs. [19,20] it is possible to generate DSs in pure 1D repulsive condensates when the tunneling rate balances the nonlinear energy of the system. For positive scattering lengths, the compensation of these two effects is not possible unless the system has a negative effective mass  $m^*$  [ $1/m^* = (1/\hbar^2)(\partial^2 E/\partial k^2)$ , where  $E$  is the energy of the first band and  $k$  its quasimomentum (see Fig. 2)]. At least two possible mechanisms can easily place the system in such a region, inverting thus the sign of the tunneling. One possibility [13] consists on providing the condensate with an external momentum to place it at the edge of the first Brillouin zone where the effective mass is negative (see Fig. 2(a)). This can be done for instance, by introducing—in the absence of the magnetic trap—a tilt in the optical lattice. A second mechanism to reach the negative effective mass region relies on the variation of the relative phase of the condensate in the lattice. Concretely, a repulsive condensate in a periodic potential with a phase difference of

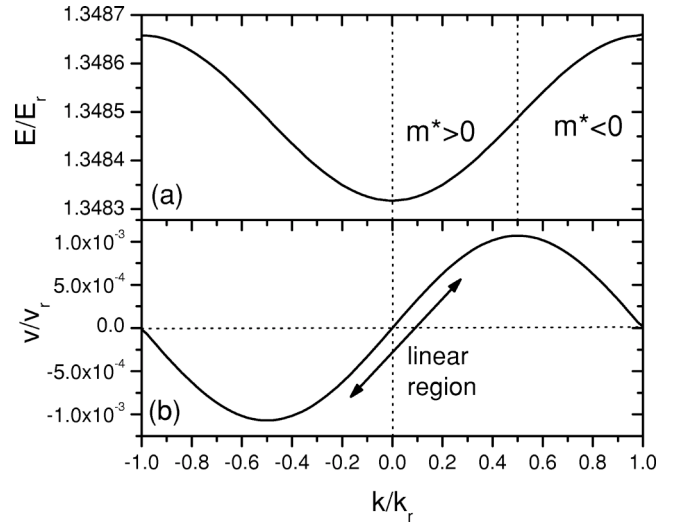


FIG. 2. (a) Energy of the first band in units of the recoil energy and (b) velocity profile in units of  $v_r = \hbar\pi/md$  as a function of the quasimomentum in the first Brillouin zone for an optical potential depth of  $8E_r$ .

$\pi$  between consecutive wells gives rise to the so-called staggered discrete soliton-type [34]. Such a phase structure can be achieved using the well established method of phase imprinting [35] which allows to modify the phase of a condensate without modifying its density profile. To this aim we propose to use a second optical lattice with double spatial period than the first one acting for a time much shorter than the characteristic times of the system, i.e., the correlation ( $\tau_c = \hbar/\mu$ ) and the tunneling ( $\tau_t = \hbar/J$ ) time. The phase imprinted in this way depends solely on the amplitude of this second standing wave and on the time in which it acts. In the following we describe in detail how the phase imprinting method is implemented. First we calculate the ground state of the system in the presence of an optical lattice. This can be done either by calculating directly (using GPE in imaginary time) the ground state of the system in the presence of both the magnetic trap and the optical lattice or by calculating the ground state of the system in the presence of the magnetic trap only and afterwards growing adiabatically the optical lattice and letting the system evolve to the new ground state. As expected both methods yield the same ground state. Once the ground state is found, a second optical lattice with an amplitude of  $72.5 E_r$  acting for  $t=0.4$  ms performs the phase imprinting while the magnetic trap is suddenly switched off. Our results are summarized in Fig. 3. Figure 3(a) shows the density profile of the ground state of the combined trap (magnetic and lattice) while Fig. 3(b) displays the density profile of the localized structure 100 ms after turning off the magnetic trap. The system evolves from the ground state shown in Fig. 3(a) to the localized structure shown in Fig. 3(b) which remains unaltered for times much longer than the tunneling time of the system. This structure contains 40% of the initial number of atoms. In Fig. 3(c), we display the phase profile corresponding to Fig. 3(b) in where clear phase jumps of  $\pi$  between consecutive sites of the optical lattice in the spatial region occupied by the localized structure are present. Finally by applying an external mo-

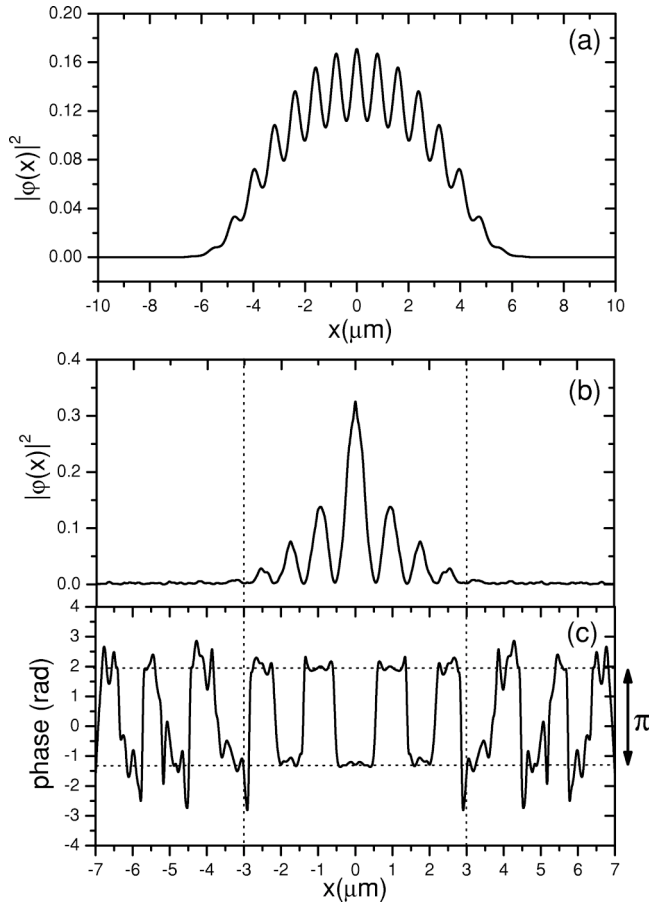


FIG. 3. (a) Density profile of the ground state of a  $^{87}\text{Rb}$  condensate in the combined (magnetic and optical) trap for  $N=2000$ ,  $\omega_x=50 \times 2\pi$  Hz,  $\omega_y=\omega_z=92 \times 2\pi$  Hz,  $a=5.8$  nm,  $V_0=1E_r$ , and  $d=0.8$   $\mu\text{m}$ . (b) Density profile of the staggered soliton 100 ms after the imprinting of a phase difference of  $\pi$  between consecutive wells and after the magnetic trap is switched off. (c) Phase profile of the staggered soliton shown in (b).

momentum to the localized structure we observe that it moves without distortion, evidencing thus that such structures correspond indeed to discrete bright solitons. Notice that the applied momentum must keep the structure in the negative effective mass region of the band [Fig. 2(a)] in order not to destroy the soliton.

We turn now to the case of negative scattering length. In continuous systems, the attractive nature of the interactions compensates the effect of the kinetic energy and, therefore, the ground state of a one-dimensional homogeneous condensate with negative scattering length is already a bright soliton. The presence of an optical lattice in such systems permits the creation of a discrete bright soliton. Thus, for a fixed number of atoms,  $N$ , one can straightforwardly vary the number of occupied sites by varying only the depth of the optical potential  $V_0$ . Since the interactions are now attractive the number of sites occupied by the discrete solitons is typically much smaller than in the case of positive scattering length. Bearing all this features in mind, it becomes clear that such systems are unique to study how the movement of a discrete soliton depends on the degree of discreteness of the structure, i.e., to observe the PN barrier [24]. We have analyzed the

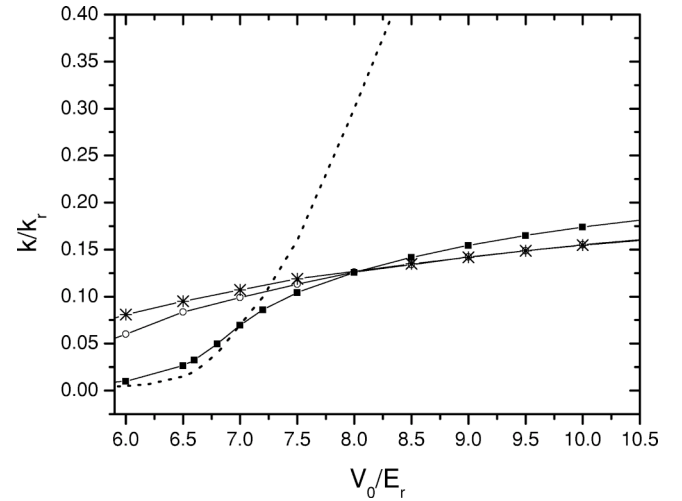


FIG. 4. Momentum associated with the PN barrier calculated with the variational method (open dots), with the imaginary time evolution of the GPE (squares), and with the DNLSE (stars). The necessary momentum to move the soliton (calculated with the real time evolution of the GPE) is displayed by the dotted line.

case of a condensate of  $^7\text{Li}$  confined in a magnetic trap with  $\omega_y=\omega_z=20 \times 2\pi$  kHz, and  $\omega_x=75 \times 2\pi$  Hz. We fix  $aN=-14$  nm [36]. Again, to analyze the generation and the propagation of discrete structures we start by calculating the ground state of the system in the combined (lattice + magnetic trap) potential. We proceed as in the case of Rubidium, either growing adiabatically the optical lattice after the ground state of the condensate in the trap has been found or by finding directly the ground state in the presence of both potentials. After the magnetic trap is switched off we observe that the localized structure remains without dispersion for times much larger than the tunneling time of the system. To study the effect of the discreteness we vary the values of the depth of the optical potential between  $6 \leq V_0/E_r \leq 10$  for a fixed lattice spacing of  $d=0.8$   $\mu\text{m}$ . The number of sites significantly occupied by the discrete structure then vary between 11 and 3.

We calculate for these sets of parameters the PN barrier, i.e., the difference in energy between the localized structure centered in a minimum of the periodic potential [Fig. 1(a)] and the structure corresponding to a lattice displaced by half lattice period [Fig. 1(b)]. To test the validity of the variational method and the validity of the tight-binding approximation, we calculate the PN barrier using the expressions developed in Sec. III and solving numerically in imaginary time the DNLSE (using a Runge-Kutta method). Then, we compare these results with the barrier obtained by solving directly the full GPE in imaginary time. The results of those calculations are summarized in Fig. 4, where we display the momentum associated with the PN barrier (in units of  $k_r$ ) as a function of the depth  $V_0$  of the optical lattice.

We observe that for large optical potential depths ( $V_0 \geq 8E_r$ ) the results obtained with the DNLSE and the variational method using the exponential ansatz match each other perfectly and agree well with those obtained by solving directly the GPE. For low optical potential depths ( $V_0 < 8E_r$ ) the DNLSE and the variational start to disagree because the

exponential ansatz becomes less appropriate as the number of sites increases. Moreover, in this region a clear disagreement between the GPE and the methods that assume tight binding appears, evidencing thus the inapplicability of the tight-binding approximation. Note that, surprisingly, the tight-binding results for the PN barrier fail to match with the GPE solution even for values of the lattice potential that are typically assumed as being well into the tight-binding regime. In this sense our calculations reveal that the PN barrier is certainly very sensitive to slight deviations from the tight-binding conditions. The latter can be explained taking into account that if the on-site dynamics inside each potential well is not completely frozen, as assumed in Eq. (3), the energy associated to the on-site movement can smear out the PN barrier.

Let us recall that physically the presence of the PN potential implies that the soliton will only move if a momentum above the critical one, determined by the PN barrier, is provided. Therefore, we perform a dynamical study by solving the GPE in real time after providing an instantaneous transfer of momentum to the structure. The latter can be achieved either via phase imprinting or by applying a linear potential during a time shorter than any other time scale. We monitor for every value of  $V_0$  the minimum applied momentum to move the localized structure. The results are displayed in Fig. 4 as a dotted line. We observe that the barrier calculated with the static GPE and the dynamical results only agree for low optical potential depths ( $V_0 < 7E_r$ ). For such cases the soliton is spread considerably in real space being, therefore, well localized in momentum space. This is the necessary condition to move the structure as a whole in the linear region of the velocity profile [Fig. 2(a)], where the velocity is proportional to the given momentum. The movement for the case of  $V_0 = 6E_r$  after a transfer of momentum of  $0.1k_r$  is depicted in Fig. 5(a). Conversely, a clear deviation from all the previous calculations of the PN barrier appears as the lattice potential depth increases. Our results show that there exist regions in which it is not possible to reach dynamically the configuration corresponding to Fig. 1(b). This is what happens for large optical potentials ( $V_0 > 8E_r$ ) where the soliton is highly localized in space and, therefore, spread in momentum. We observe that for ( $V_0 \geq 10E_r$ ), no motion is found no matter how large is the initial momentum given to the soliton. In this case, the width in momentum space of the localized structure is of the order of the momentum of the lattice, i.e., the first Brillouin zone is saturated and the movement is prevented. For intermediate optical potentials ( $8 - 9E_r$ ), we observe that movement of these structures is not possible in the linear part of the velocity profile (Fig. 2) even if one overcomes the PN barrier. Nevertheless, if the given momentum is large enough, we observe in our simulations a reorganization of the structure which allows it to move by losing first a fraction of the atoms and spreading afterwards in space, being later on enough localized in momentum space to move as a whole [Fig. 5(b)]. The rearranged structure exhibits a complex dynamics as a result of the interplay between nonlinearity and band structure.

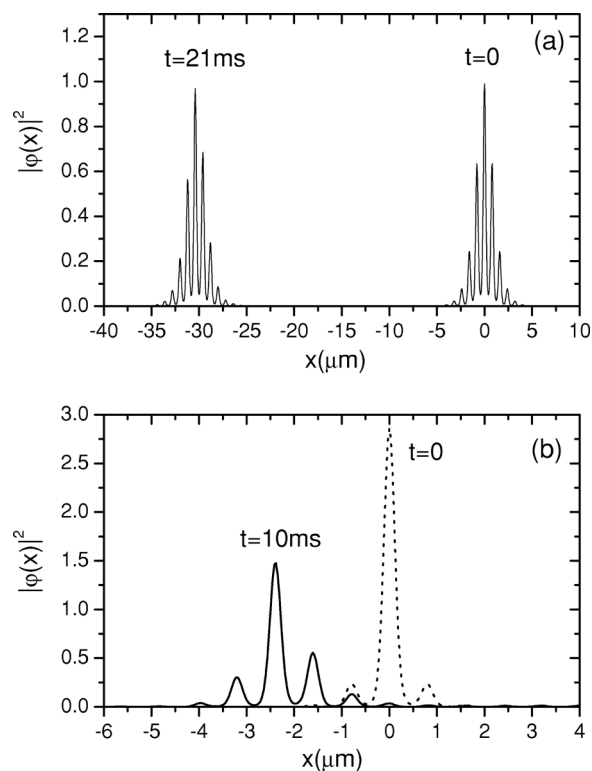


FIG. 5. (a) Density profile of a discrete soliton created in the presence of an optical potential of depth  $6E_r$  before and 21 ms after a transfer of momentum of  $0.1k_r$  is applied to the structure. (b) Density profile of the localized structure generated with a lattice of amplitude  $8E_r$  (dotted line) and the corresponding density profile 10 ms after a kick of  $0.3k_r$  is given (solid line). Seventy-seven percent of the atoms remain in the reconfigured structure.

## V. CREATION OF TWO- AND THREE-DIMENSIONAL SELF-TRAPPED STRUCTURES

In this section, we briefly address the experimental possibilities for the generation of discrete solitons in higher spatial dimensions in attractive condensates [22,23]. From the variational ansatz discussed in Sec. III, it is possible to obtain that two- and three-dimensional self-trapped structures may be stable provided that the ratio  $|J/U|$  is low enough. The threshold value for the 2D case is 0.175(0.2) and for the 3D case 0.13(0.15) using an exponential (Gaussian) ansatz. The limitation to such low tunneling rates imposes a restriction in the maximal number of sites occupied by the localized structure.

We consider the full 3D case with an spherical magnetic trap and we address the creation of 3D localized structures in the presence of a 2D or 3D optical lattice. Notice that due to the attractive interactions, the possibility of collapse imposes some restrictions in the number of atoms and in the features of the optical lattice. In some situations, even if the collapse in the magnetic trap is prevented, the adiabatic growing of the lattice leads to the on-site collapse. This effect must be taken into account if the 3D localized structures are to be created. A condensate of  ${}^7\text{Li}$  with  $aN = -70$  nm and initially in a spherical magnetic trap of frequencies  $\omega_x = \omega_y = \omega_z = 375 \times 2\pi$  Hz has been considered. This situa-

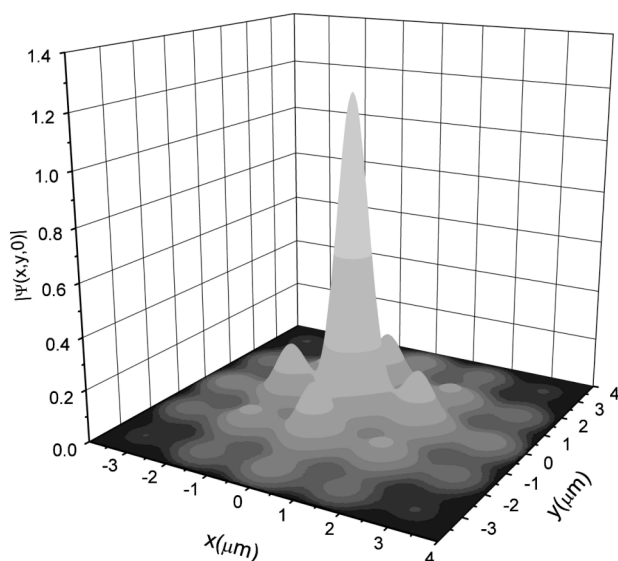


FIG. 6. Spatial structure of a matter discrete localized structure created in the presence of a 3D optical lattice with a depth  $V_0=6E_r$ , and a period  $d=1.6 \mu\text{m}$ , as a function of two spatial coordinates,  $(x,y)$ , for a fixed value of the third coordinate,  $z=0$ .

tion corresponds for instance to  $N=500$   $^7\text{Li}$  atoms and a modified  $s$ -wave scattering length  $a=-0.14$  nm available with Feshbach resonances [5,6]. Figure 6 displays the spatial structure of a matter discrete localized structure created in the presence of a 3D optical lattice with period  $d=1.6 \mu\text{m}$ , and  $V_0=6E_r$ . Therefore, the discreteness of the lattice potential allows for the interesting possibility of a controllable generation of a self-trapped regular 3D BEC structure. Unfortunately, the restriction in the number of sites occupied in the localized structures created in the two- and three-dimensional cases, imposes a severe limitation for their mobility. As already discussed for the 1D case, the spread in momentum space of these structures prevents their motion, at least in the linear region of the band structure.

## VI. CONCLUSIONS

We have analyzed the conditions to generate discrete solitons in 1D Bose-Einstein condensates, either with positive or

negative scattering length. In particular, in repulsive interacting condensates, the phase imprinting method has been proposed to controllably create bright staggered type solitons. Once generated, we have addressed the mobility of these structures. This mobility is characterized by two different effects: (i) the presence of the PN barrier, a purely discrete effect which sets a minimal kinetic energy to move half a lattice period, and (ii) the spreading of the atomic wave function in momentum space due to the spatial localization in few lattice sites. The mobility is only possible if the PN barrier is overcome, but even if this is the case a clear soliton motion is only possible if the system is placed in a region of linear dispersion. Our analysis shows that the estimation of the PN barrier is crucially sensitive to slight deviations from the tight-binding conditions. In particular, the tight-binding approximation has been shown to fail significantly for large lattice potentials which are typically assumed to guarantee the validity of such an approximation.

The mobility of discrete solitons generated in this way offer interesting possibilities in the context of BEC guiding. In this sense similar ideas as those analyzed in the case of optical DS [37] could be employed to generate DS networks, which could constitute an (nondispersive) approach to the issue of integrated atom optics.

Finally, we have shown that the discreteness of the lattice also allows for self-trapped structures in 2D and 3D. Due to the strong localization required, their mobility is prevented to a large extent. These higher-dimensional structures could open alternative routes to optical tweezers [38] and magnetic conveyor belts [39], for the storing, manipulation, and transport of atomic condensates.

## ACKNOWLEDGMENTS

We acknowledge support from Deutsche Forschungsgemeinschaft (SFB 407), the RTN Cold Quantum Gases, ESF PESC BEC2000+, and the Ministero dell'Istruzione, dell'Università e della Ricerca (MIUR). V.A. acknowledges support from the European Community (HPMF-CT-2002-01847). L.S. and P.P. wish to thank the Alexander von Humboldt Foundation, the Federal Ministry of Education and Research, and the ZIP Programme of the German Government.

- 
- [1] M. H. Anderson *et al.*, *Science* **269**, 198 (1995); K. B. Davis *et al.*, *Phys. Rev. Lett.* **75**, 3969 (1995); C. C. Bradley *et al.*, *ibid.* **75**, 1687 (1995); C. C. Bradley, C. A. Sackett, and R. G. Hulet, *ibid.* **78**, 985 (1997).
- [2] P. Meystre, *Atom Optics* (Springer-Verlag, New York, 2001).
- [3] S. Burger *et al.*, *Phys. Rev. Lett.* **83**, 5198 (1999).
- [4] J. Denschlag *et al.*, *Science* **287**, 97 (2000).
- [5] L. Khaykovich *et al.*, *Science* **296**, 1290 (2002).
- [6] K. E. Strecker *et al.*, *Nature (London)* **417**, 150 (2002).
- [7] E. A. Donley *et al.*, *Nature (London)* **412**, 295 (2001).
- [8] B. P. Anderson and M. A. Kasevich, *Science* **282**, 1686 (1998).
- [9] O. Morsch *et al.*, *Phys. Rev. Lett.* **87**, 140402 (2001).
- [10] F. S. Cataliotti *et al.*, *Science* **293**, 843 (2001).
- [11] M. Greiner *et al.*, *Nature (London)* **415**, 39 (2002).
- [12] A. Smerzi *et al.*, *Phys. Rev. Lett.* **89**, 170402 (2002); F. S. Cataliotti *et al.*, *New J. Phys.* **5**, 71 (2003).
- [13] B. Eiermann *et al.*, *Phys. Rev. Lett.* **91**, 060402 (2003).
- [14] O. Zobay *et al.*, *Phys. Rev. A* **59**, 643 (1999).
- [15] Gap solitons have been recently observed at the University of Konstanz, M. Oberthaler (private communication).
- [16] D. N. Christodoulides and R. I. Joseph, *Opt. Lett.* **13**, 794 (1988).
- [17] H. S. Eisenberg *et al.*, *Phys. Rev. Lett.* **81**, 3383 (1998).

- [18] J. W. Fleischer *et al.*, Phys. Rev. Lett. **90**, 023902 (2003).  
[19] A. Trombettoni and A. Smerzi, Phys. Rev. Lett. **86**, 2353 (2001).  
[20] F. Kh. Abdullaev *et al.*, Phys. Rev. A **64**, 043606 (2001).  
[21] P. J. Y. Louis *et al.*, Phys. Rev. A **67**, 013602 (2003).  
[22] E. A. Ostrovskaya and Y. S. Kivshar, Phys. Rev. Lett. **90**, 160407 (2003).  
[23] B. B. Baizakov, B. A. Malomed, and M. Salerno, Europhys. Lett. **63**, 642 (2003).  
[24] See Y. S. Kivshar and D. K. Campbell, Phys. Rev. E **48**, 3077 (1993) and references therein.  
[25] J. W. Fleischer *et al.*, Nature (London) **422**, 147 (2003).  
[26] K. Berg-Sorensen and K. Mølmer, Phys. Rev. A **58**, 1480 (1999).  
[27] J. Javanainen, Phys. Rev. A **60**, 4902 (1999).  
[28] D. I. Choi and Q. Niu, Phys. Rev. Lett. **82**, 2022 (1999).  
[29] M. L. Chiofalo, S. Succi and M. P. Tosi, Phys. Rev. A **63**, 063613 (2001).  
[30] M. Krämer, L. Pitaevskii, and S. Stringari, Phys. Rev. Lett. **88**, 180404 (2002).  
[31] P. Pedri *et al.*, Phys. Rev. Lett. **87**, 220401 (2001).  
[32] M. Olshanii, Phys. Rev. Lett. **81**, 938 (1998).  
[33] W. Zwerger, J. Opt. B: Quantum Semiclassical Opt. **5**, 9 (2003).  
[34] Y. S. Kivshar, Opt. Lett. **18**, 1147 (1993).  
[35] Ł. Dobrek *et al.*, Phys. Rev. A **60**, R3381 (1999).  
[36] Notice that in the simulations the fixed parameter is Na and therefore, a certain freedom in the choice of the number of atoms and *s*-wave scattering length exists. Note that the scattering properties of <sup>7</sup>Li can be strongly modified by the use of Feshbach resonances [5,6].  
[37] D. N. Christodoulides and E. D. Eugenieva, Phys. Rev. Lett. **87**, 233901 (2001).  
[38] T. L. Gustavson *et al.*, Phys. Rev. Lett. **88**, 020401 (2002).  
[39] M. Greiner *et al.*, Phys. Rev. A **63**, 031401 (2001).